Upper-Ocean Eddy Transports of Heat, Potential Vorticity, and Volume in the Northeastern North Atlantic—"Vivaldi 1991"

H. LEACH, S. J. BOWERMAN, AND M. E. MCCULLOCH*

Oceanography Laboratories, University of Liverpool, Liverpool, United Kingdom

(Manuscript received 16 April 2001, in final form 11 April 2002)

ABSTRACT

Mesoscale eddies in the northeast North Atlantic were investigated using the SeaSoar towed CTD and ADCP data from the 1991 *Vivaldi* cruise. These data cover an area of 1700 km × 1500 km between 39° and 54°N and between 35° and 10°W. To maximize statistical significance, but retain the possibility of determining north–south gradients, statistics of eddy quantities were calculated separately for the northern and southern halves of the cruise area. The mean flow in the south is essentially zero; in the north the flow is dominated by the North Atlantic Current (NAC) with a mean speed of 6.5 cm s^{-1}. The eddy kinetic energy in the south, 205 cm^2 s^{-2}, is, however, only slightly less than in the north, 272 cm^2 s^{-2}. The eddy momentum transports, or Reynolds stresses, $\overline{u'v'}$, show a poleward decrease, corresponding to an acceleration of the mean eastward flow associated with the NAC of 0.03 cm s^{-1} day^{-1}. The eddy heat transports, $\overline{\mathbf{u}'T'}$, are not significantly different from zero in the south but show a clear poleward transport in the north of 5.5 K cm s^{-1}, or 0.1 PW for the 365-m layer 1500 km wide. The depth-averaged eddy potential vorticity fluxes, $\overline{\mathbf{u}'q'}$, show a convergence toward the source region of the low-potential-vorticity eastern North Atlantic Central Water west of Biscay. The residual or rectified eddy transport velocity implied by the eddy potential vorticity flux, $\mathbf{u}^* = -\overline{\mathbf{u}'q'}/\overline{q}$, is 0.7 cm s^{-1} toward the southwest in the south, while in the north it is 0.9 cm s^{-1} toward the northwest crossing the property isolines. The directions correspond to a divergence from the formation region of the eastern North Atlantic Central Water. An assessment of the overall volume transport of the region suggests that the westward eddy volume transport (~4 Sv; Sv ≡ 10^6 m^3 s^{-1}) is almost balanced by an eastward geostrophic flow (~3 Sv) with the remainder being supplied by a smaller contribution leaving the northward-flowing eastern boundary current (~1 Sv).

1. Introduction

Mesoscale eddies transport heat, freshwater, momentum, potential vorticity, and mass and are therefore responsible for an irreversible movement of properties and mass in addition to that effected by the mean flow. Recently there has been considerable increase in interest in the role played by eddies in the ocean and their effect on the general circulation with considerable effort expended to find parameterizations for them, made famous by Gent and McWilliams (1990). While there has been much work on measuring eddy kinetic energy, particularly using satellite altimetry, there has been less on the other quadratic quantities that are key to the role of the eddies. In this paper we report on the analysis of a large-area high-resolution survey, which can contribute observations of these quantities to the discussion.

The hydrography and current system of the northeastern North Atlantic has been the subject of study for a long time and a number of authors over the years have published various interpretations (see, e.g., Helland-Hansen and Nansen 1926; Dietrich et al. 1975; Krauss 1986; Ellett 1993). Though in some important details these authors differ, they all describe a North Atlantic Current (NAC) that crosses the Mid-Atlantic Ridge at about 51°N and turns north before 20°W. South of this only Dietrich et al. (1975) show a major current turning southward and flowing between the Azores and Iberia, and that is based on geostrophic calculations relative to the rather shallow reference level of 1000 m. Paillet and Mercier (1997) also show a weak southward flow in this region. The other authors generally show the region south of the NAC to have insignificant mean currents. Indeed, recently several authors have suggested that there may even be a mean westward flow in the region of the Azores (Onken 1993; Cromwell et al. 1996; Bowerman and Leach 1997). In a detailed study of the upper-ocean hydrographic data from the same cruise as used in this study Pollard et al. (1996) have described a region of mode water formation west of Biscay. They identify this saline mode water as eastern North Atlantic Central

* Current affiliation: Met Office, Bracknell, Berkshire, United Kingdom.

Corresponding author address: Dr. Harry Leach, Oceanography Laboratories, The University of Liverpool, Bedford Street North, Liverpool L69 7ZL, United Kingdom.
E-mail: leach@liverpool.ac.uk

Water and describe how, on purely hydrographic grounds, it must spread out toward the west.

The variability of flow in the ocean is usually represented by the eddy kinetic energy (EKE) derived either from drifting buoys (e.g., Richardson 1983; Krauss and Käse 1984) or from satellite altimeter data (e.g., Heywood et al. 1994). Within our area of interest there is a wide range of EKE from the active region of the North Atlantic Current in the northwest to the area of relatively weak eddies west of Iberia. On the basis of satellite altimetry it has been possible to show that there is seasonal variability in the EKE with a maximum following the wind stress curl maximum (White and Heywood 1995; Stammer and Wunsch 1999). This had led to the conclusion that in regions away from strong mean currents eddies may be forced by the wind rather than by baroclinic instability of the mean flow. Our single snapshot from the spring of 1991 cannot directly contribute to this discussion, though our EKE is consistent with other observations.

Generally regions of high EKE are equated to regions of strong mean flow. Indeed, Heywood et al. (1994) advocate using the EKE to identify the position of current bands. However, Bowerman and Leach (1997) in a study of the region north of the Azores show that the EKE may have a different distribution to the mean flow or eddy transport parameters. It is these eddy transports, rather than the EKE, that describe the contribution made by eddies to irreversible processes.

Eddy transports were first considered in zonal atmospheres (Edmon et al. 1980) and later extended to 3D atmospheric flows (e.g., Hoskins et al. 1983). These ideas have been more recently extended to the ocean. Lee and Leach (1996) using a model and Bowerman and Leach (1997) using in situ data have confirmed that in the ocean, as in the atmosphere, the heat transport by eddies dominates their role in momentum transport and that the residual circulation driven by the eddies can be a significant fraction of the mean geostrophic flow and at right angles to it. Lee et al. (1997) have described how eddies can effect a net transfer of mass and tracers in a baroclinicly unstable flow. Basically there is a correlation between the velocity fluctuations, $\mathbf{u}' = \mathbf{u} - \overline{\mathbf{u}}$, and the isopycnic layer thickness fluctuations, $h' = h - \overline{h}$, such that a rectification occurs leading to a residual velocity $\mathbf{u}^* = \overline{\mathbf{u}'h'}/\overline{h}$, which implies a net volume transport. The sense of the net volume transport is such that it tends to flatten the isopycnals so that (in the Northern Hemisphere) it will be to the left of the mean flow near the surface and to the right at depth. Other authors (Treguier et al. 1997; Marshall et al. 1999) have tended to argue that it is more correct to use the potential vorticity rather than the layer thickness. While there is a considerable body of literature discussing these transports in model calculations, there have so far been few attempts to calculate them from observations.

The hydrographic structure from the SeaSoar sections

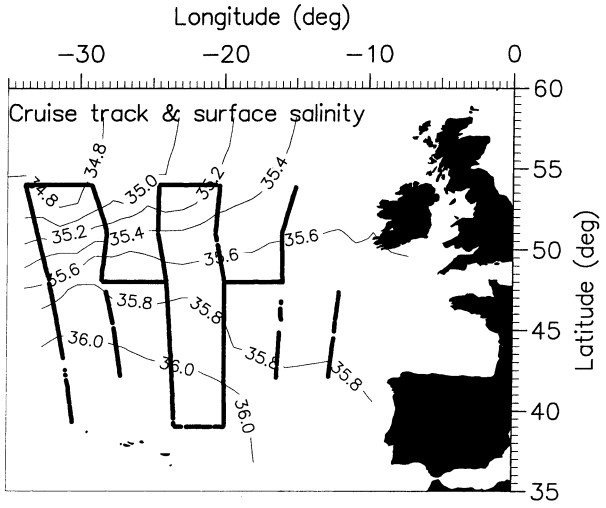

FIG. 1. The ''Vivaldi 1991'' cruise track superimposed on the mean surface salinity. The core of the North Atlantic Current roughly follows the 35.2 isohaline, with the lower salinities of the subpolar gyre to the NW and the higher salinities of the subtropical gyre to the SE. For the purpose of calculating the statistics the data were split along 48°N, the latitude of the repeat sections, with the repeats themselves being distributed equally, westbound to the southern half, eastbound to the northern half.

alone from this dataset has been considered in detail by Pollard et al. (1996). The philosophy of the present paper is to extend their analysis by combining the hydrographic and current data in a statistical analysis to investigate the role of eddies in the upper ocean in the general circulation of this area.

The region discussed in this paper is a region of strong air–sea interactions that give rise to the mode water known as the eastern North Atlantic Central Water and forms the theme of Pollard et al.'s (1996) paper. However our survey took place in the spring during a period of net heat gain in the surface layer. The mixed layer depth was on average 29 m deep and so did not interfere with the processes discussed here. The air–sea interactions in this region during the experiment are discussed by McCulloch and Leach (1997).

2. Data and methods

In the spring of 1991 upper-ocean data were collected during Cruises 58 and 59 of RRS *Charles Darwin* (Pollard et al. 1991) along six parallel quasi-meridional sections between 35° and 10°W in the northeastern North Atlantic (Fig. 1). The sections were 300 km apart zonally and stretched from 39° to 54°N. The fourth section from the west ran along 20°W. These data cover an area of 1700 km north–south × 1500 km east–west. Hydrographic data in the upper 500 m were collected using a Neil Brown Mark 3 CTD mounted in a SeaSoar towed vehicle. In practice the data density became rather sparse below 365 m, so this was the greatest depth that could be used in our analysis. Current data were collected

using an RDI 150-kHz ADCP combined with GPS navigation. (Enhanced positional accuracy of ±7 m was available at the time due to lack of signal degradation for the purpose of the Gulf War earlier in the year.) Every round 3° of latitude a supporting top-to-bottom CTD cast was made. The SeaSoar CTD data and ADCP data were interpolated to a standard spacing of 4 km in the horizontal and 8 m in the vertical. The data calibration and processing are described by Cunningham et al. (1992) and Griffiths et al. (1992).

For this paper, the eddy transports for the northern (39°–48°N) and southern (48°–54°N) halves (Fig. 1) of the whole survey area were calculated in order to maximize statistical significance but still be able to consider meridional changes. Values quoted for the northern and southern halves of the area have been averaged over these halves and fluctuations calculated for each of these halves separately by subtracting these means from the data for each half. In other words, in the context of this paper the word ''eddy'' means deviation from the mean value calculated over the northern or southern half of our cruise area, 700 km × 1500 km for the north, 1000 km × 1500 km for the south. The values along the repeated 48°N sections were split between the two halves with the outbound, west-going values attributed to the southern half and the inbound, east-going values attributed to the northern half. Values shown at higher resolution have been averaged in 3° latitude × 300 km longitude boxes, as was done by Bowerman and Leach (1997), and deviations from these means then constitute eddies.

The potential vorticity q is defined as

$$q = -\frac{f}{\rho_0}\frac{\partial \sigma_\theta}{\partial z},$$

where f is the Coriolis parameter, ρ_0 a reference density, and $\partial\sigma_\theta/\partial z$ the vertical gradient of potential density. This had to be calculated in depth coordinates as using density surfaces proved impractical for the relatively thin 365-m layer of data in which density surfaces outcropped or were lost from the bottom of the layer within the area of averaging. Admittedly the relative vorticity has been neglected in the calculation of potential vorticity, but Fischer et al. (1989), in a mesoscale study in the NAC, show that terms involving relative vorticity only contribute about 9% to the variance of the potential vorticity.

3. Results

a. Mean conditions

The mean hydrographic conditions in the area investigated are best illustrated by the mean surface salinity (Fig. 1). Surface salinity is not subject to significant seasonal change over the period of the expedition. [Josey et al. (1999) give a net flux of about 8 mm month^{-1}, which implies a salinity change of only 0.01 in six weeks for a layer of 50 m.] The strongest gradients are seen at 51°N on the western boundary, where the North Atlantic Current enters the region. In the NW corner of the area are seen the freshest waters of the subpolar gyre with salinities less than 35.3 psu. The isohalines fan out toward the east but the curving of the NAC to the north can be seen too.

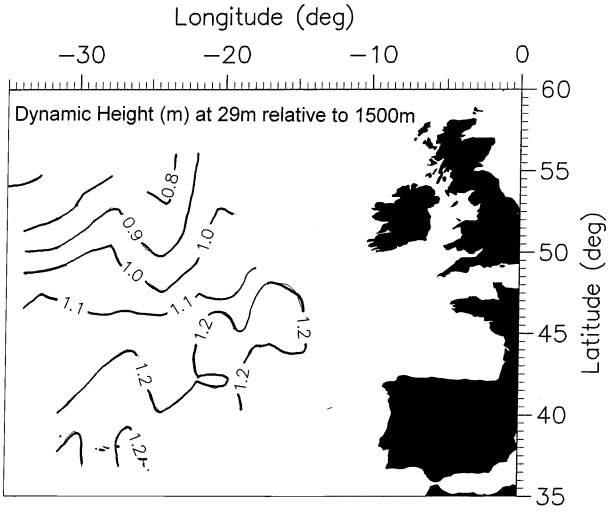

FIG. 2. Dynamic height at 29 m relative to 1500 m calculated from the sparse CTD survey. Units are meters of dynamic height. The NAC enters at the western boundary at about 51°N and leaves at the northern boundary at about 20°W. The SE part of the region shows little flow. The dynamic height difference across the NAC corresponds to a speed of 5 cm s^{-1}.

The dynamic height at 29 m relative to 1500 m is shown in Fig. 2. This was calculated from the deep CTD casts that were made at every 3° of latitude along the tracks shown in Fig. 1. Again the NAC can be seen entering the domain at about 51°N and leaving at about 20°W. The dynamic height difference across the NAC corresponds to a speed of about 5 cm s^{-1}. The mean flow from the ADCP averaged over the top 365 m in the southern half of the area is small, (-0.2 ± 0.7, -0.1 ± 0.8) cm s^{-1}, and not significantly different from zero in the *t*-test sense, while in the northern half of the area the flow of the NAC has a mean velocity of (5.2 ± 0.8, 3.9 ± 0.8) cm s^{-1} or 6.5 cm s^{-1} to 053°. The mean flow as a function of depth is shown in Fig. 3. The flow in the north is to the east and north decreasing with depth, while the flow in the south is zero. Extrapolating the flow in the north down by linear regression excluding the shallowest value, which might be contaminated by Ekman flow, gives zero-crossing depths for $\overline{u}$ of 580 ± 80 m and for $\overline{v}$ of 780 ± 90 m.

b. Eddy kinetic energy

Eddy transports form the focus of this paper, but the data naturally allow the calculation of eddy kinetic energy too, though there are superior datasets based, for example, on satellite altimetry. The mean eddy kinetic

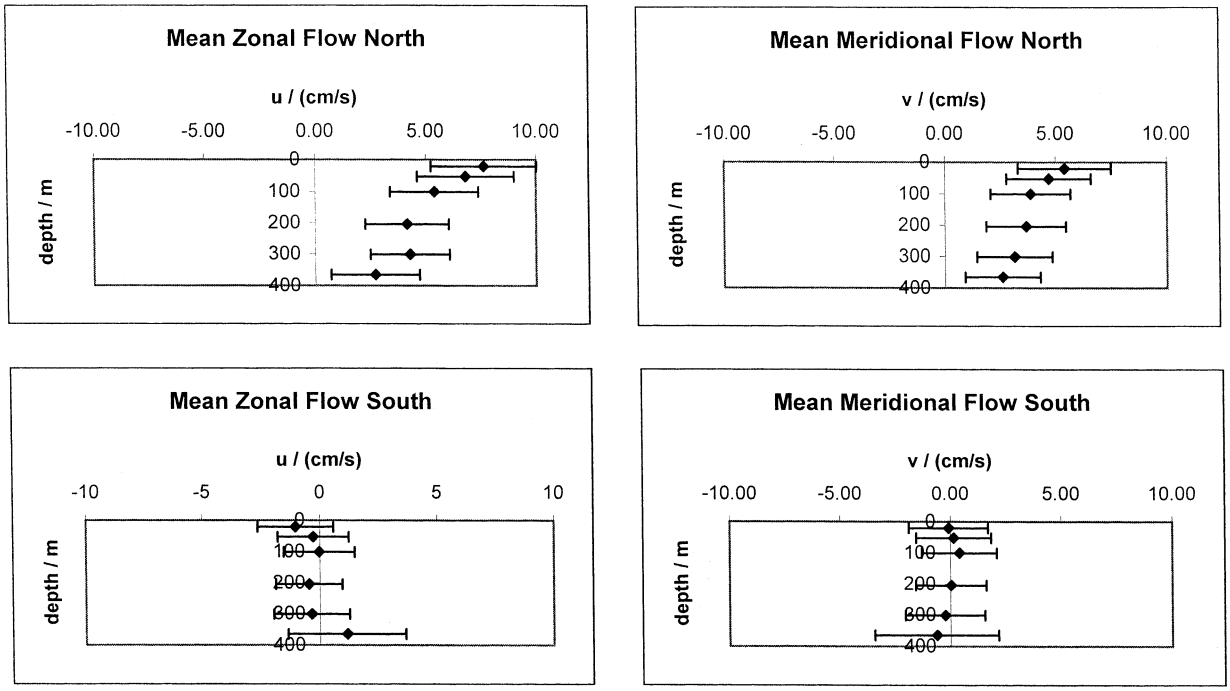

FIG. 3. Profiles of the mean flow as a function of depth showing both u and v components for the northern and southern halves of the area. The flow in the north shows eastward and northward flow decreasing with depth. The flow in the south is essentially zero. Extrapolating the flow in the northern half down by linear regression excluding the shallowest value, which might be contaminated by Ekman flow, gives zero-crossing depths for $\overline{u}$ of 580 ± 80 m and for $\overline{v}$ of 780 ± 90 m.

energy [EKE = $\frac{1}{2}(\overline{u'^2} + \overline{v'^2})$] for the top 365 m in the northern half of our region is 272 ± 11 cm^2 s^{-2} and for the southern half it is 205 ± 9 cm^2 s^{-2}. A map of the EKE at the top of the thermocline (53 m) is shown in Fig. 4. This shows a maximum in the region of the NAC. This picture is to some extent different to the Sea Rover dataset (Bowerman and Leach 1997), which shows the maximum EKE farther to the west with a hint of a secondary maximum in the east. The EKE decays with depth as shown by the vertical profiles of average EKE for the northern and southern halves in Fig. 5. The slightly disproportionate top value may be due to other phenomena such as inertial oscillations. While the mean flow in the south is essentially zero both in the *t*-test sense and also compared to the north, which is dominated by the North Atlantic Current, the eddy kinetic energy in the south is about 75% of the EKE in the north. Seen globally, the values in our area are not large. Peak values in western boundary currents exceed 1000 cm^2 s^{-2}, but our values are consistent with those of other authors such as Krauss and Käse (1984), Brügge (1995), White and Heywood (1995), and Stammer and Wunsch (1999). A number of these authors show particularly low values west of Cape Finisterre, not much more than 100 cm^2 s^{-2}. Müller and Frankignoul (1981) considered wind forcing to be responsible for the background EKE away from regions of strong currents instead of the baroclinic instability, and White and Heywood (1995) claim that the seasonality of the EKE signal in these areas supports this hypothesis.

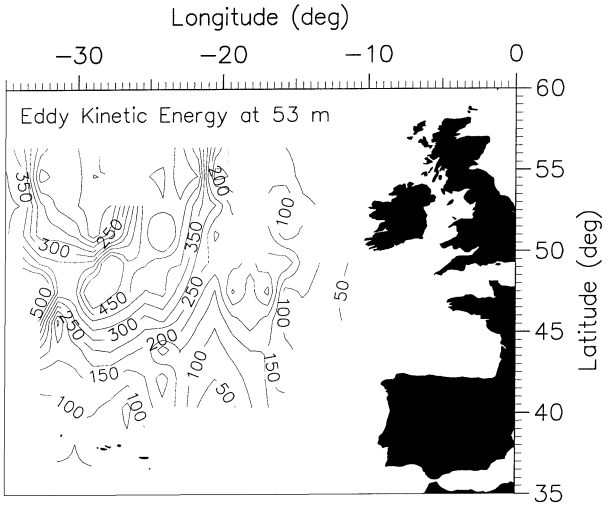

FIG. 4. Map of EKE (in units of cm^2 s^{-2}) at 53 m based on ADCP data. Values are based on variances relative to the mean flow in 300 km zonal × 3° lat boxes [as used by Bowerman and Leach (1997)]. This shows maximum values of 500 cm^2 s^{-2} in the North Atlantic Current and minimum values of 50 cm^2 s^{-2} in the SE.

Data from various techniques used in the Tourbillon Experiment (Le Groupe Tourbillon 1983) show the EKE in the eastern North Atlantic decaying to a small value, say less than 10 cm^2 s^{-2}, at depths between 1000 and 2000 m. Ignoring our shallowest values, which may be

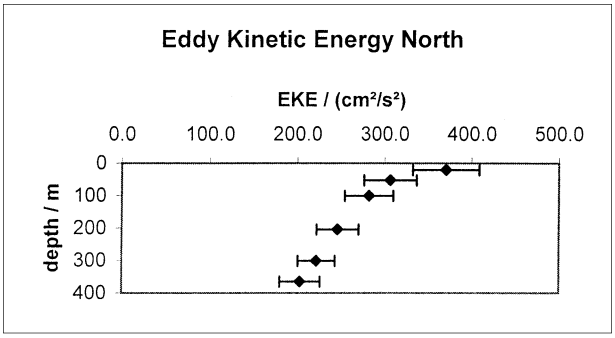

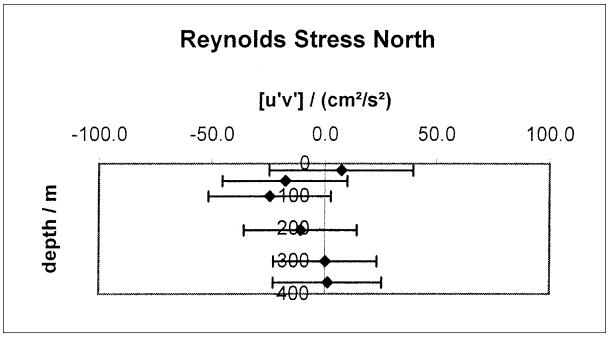

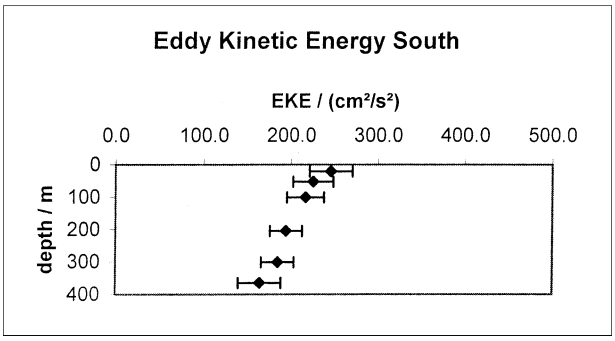

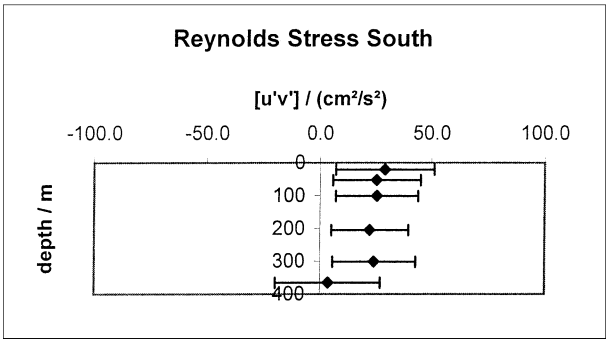

FIG. 5. Profiles of EKE (in units of $cm^2\ s^{-2}$) for the northern and southern halves of the area. The top values look disproportionately large, which may be due to phenomena other than mesoscale eddies such as inertial oscillations in the surface layer. Extrapolating the remaining values linearly downward gives zero-crossings of 980 ± 50 m and 1240 ± 90 m for the northern and southern halves of the area, respectively.

FIG. 6. Profiles of the Reynolds stress, $\overline{u'v'}$, (in units of $cm^2\ s^{-2}$) for the northern and southern halves of the area. Little vertical structure can be distinguished, but the essentially zero depth-averaged value in the north ($-7 \pm 11\ cm^2\ s^{-2}$) contrasts with the generally positive depth-averaged value in the south ($22 \pm 8\ cm^2\ s^{-2}$). The acceleration corresponds to 0.03 ± 0.02 cm s^{-1} day^{-1}. The contribution to the momentum equations, $f^{-1}\partial\overline{u'v'}/\partial y$, gives a value of -0.003 ± 0.002 cm s^{-1}.

affected by other phenomena, and extrapolating the remaining values linearly downward gives zero-crossings of 980 ± 50 m and 1240 ± 90 m for the northern and southern halves of our area, respectively. This indicates that the vertical structure of our EKE is in reasonable accord with other observations.

c. *Eddy transports of momentum, heat, potential vorticity, and volume*

For the top 365 m the average eddy momentum transports, or Reynolds stress, $\overline{u'v'}$, in the south is $22 \pm 8\ cm^2\ s^{-2}$, while in the north it is $-7 \pm 11\ cm^2\ s^{-2}$. Vertical profiles of the Reynolds stresses for the northern and southern halves of the area are shown in Fig. 6. The stresses show a poleward decrease. The Reynolds equation for the acceleration of the eastward mean flow includes a term involving the poleward gradient of the Reynolds stress $\overline{u'v'}$,

$$\frac{\partial \overline{u}}{\partial t} = \cdots - \frac{\partial \overline{u'v'}}{\partial y} \cdots,$$

so that a poleward decrease in $\overline{u'v'}$ corresponds to an acceleration of the mean eastward flow $\overline{u}$ associated with the NAC. This poleward decrease of Reynolds stress associated with eastward mean currents has also been reported by Bowerman and Leach (1997) for the NAC and by Tai and White (1990) for the Kuroshio. This structure is well known in the tropospheric jets (Leach 1984; James 1994). Apart from the generally different values of Reynolds stress in the two halves of our area, it is difficult to discern a vertical structure from Fig. 6. The acceleration corresponds to 0.03 ± 0.02 cm s^{-1} day^{-1}. The contribution to the momentum equations, $f^{-1}\partial\overline{u'v'}/\partial y$, gives a value of -0.003 ± 0.002 cm s^{-1}, which is an order of magnitude smaller than the values reported by Bowerman and Leach (1997), but here we have averaged more broadly.

The eddy heat transports, $\overline{\mathbf{u}'T'}$, at depth 101 m, superimposed on the mean surface temperature field, are shown in Fig. 7. In the south they are (0.1 ± 1.2, 0.1 ± 1.7) K cm s^{-1} and are not significantly different from zero. In the north they are (0.5 ± 2.7, 5.5 ± 2.5) K cm s^{-1} and show a clear poleward transport. Profiles of eddy heat transport are shown in Fig. 8. The zonal transports show no significant values except, marginally, at 365 m in the north. The meridional transport shows poleward values in the thermocline in the north, but in the south there is no significant transport. This is largely in agreement with Bowerman and Leach's (1997) results that show signs of a westward and northward eddy heat

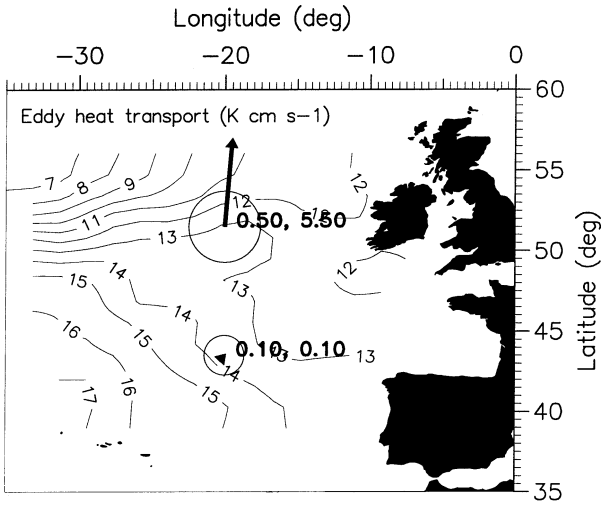

FIG. 7. The eddy heat transports, $\overline{\mathbf{u}'T'}$, (in units of K cm s^{-1}) for the northern and southern halves of the area at depth 101 m superimposed on the mean surface temperature field. In the south they are (0.1 ± 1.2, 0.1 ± 1.7) K cm s^{-1} and are not significantly different from zero. In the north they are (0.5 ± 2.7, 5.5 ± 2.5) K cm s^{-1} and show a significant poleward transport. The depth-averaged poleward heat transport for the northern area, 4.4 (±1.1) K cm s^{-1}, corresponds to 0.1 PW for the 365-m-deep layer 1500 km wide.

transport in the thermocline in the NAC but not in the mixed layer or outside the NAC. Their values are for temporal rather than spatial averages and show effectively zero meridional eddy heat transport in the mixed layer and 8 ± 8 K cm s^{-1} in the thermocline in the region of the NAC. Their errors are large, so their results are formally not inconsistent with ours. Their thermocline value is certainly within the error of our northern-area thermocline value. Bearing in mind that our northern area extends into more quiescent regions than considered in their time average, their 8 K cm s^{-1} compared to our 5 K cm s^{-1} would be understandable. The depth-averaged poleward heat transport for our northern area, 4.4 (±1.1) K cm s^{-1} corresponds to 0.1 PW for the 365-m deep layer 1500 km wide. The total poleward heat transport for this latitude is about 0.4 PW (Isemer et al. 1989). While the choice of depth range and ocean width are arbitrary for our estimate and the errors in $\overline{v'T'}$ are not small, it does give an idea of the potential size of this effect.

Another way of looking at the eddy heat transport is to consider the divergence between the northern and southern halves of our area. A simple calculation of the eddy heat flux divergence,

$$Q = \rho c_p \frac{\partial \overline{v'T'}}{\partial y} H,$$

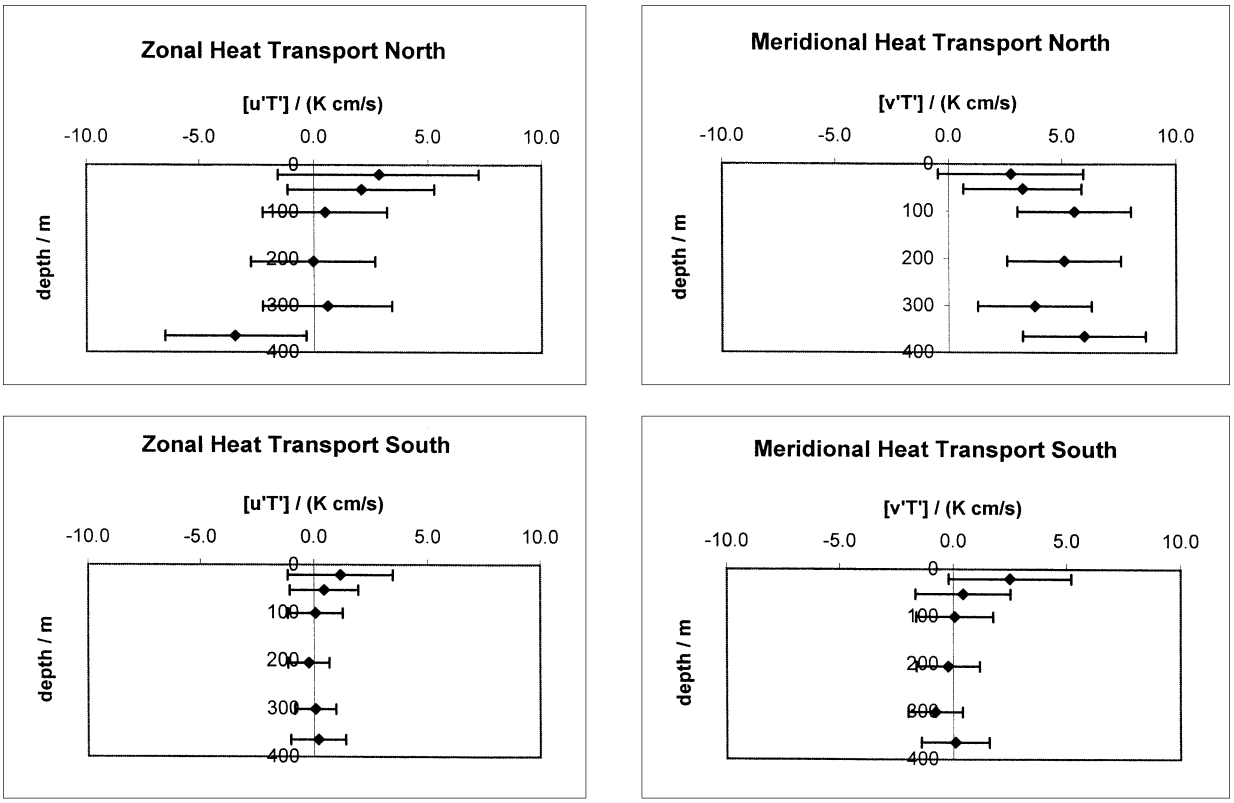

FIG. 8. Depth profiles of zonal and meridional eddy heat transport, $\overline{\mathbf{u}'T'}$, for the northern and southern halves of the area in units of K cm s^{-1}. The zonal transports show no significant values except, marginally, at 365 m in the north. The meridional transport shows poleward values in the thermocline in the north, but in the south there is no significant transport.

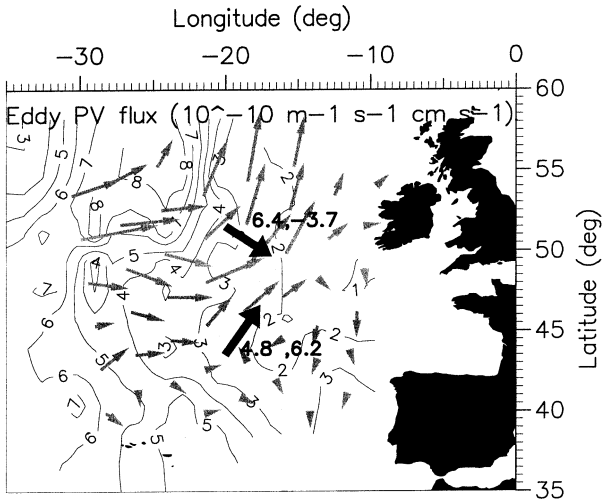

FIG. 9. The eddy potential vorticity fluxes, $\overline{\mathbf{u}'q'}$, where $q = -(f/\rho_0)(\partial\sigma_\theta/\partial z)$ (in units of 10^{-10} m^{-1} s^{-1} cm s^{-1}), averaged over the top 365 m, calculated by combining the SeaSoar CTD and ADCP data, and superimposed on the mean potential vorticity (in units of 10^{-10} m^{-1} s^{-1}) and surface geostrophic velocity fields relative to 1500 m (McCulloch and Leach 1997). In the north the flux is (6.4 ± 6.7, −3.7 ± 4.6) × 10^{-10} s^{-1} m^{-1} cm s^{-1} and in the south it is (4.9 ± 6.3, 6.2 ± 6.6) × 10^{-10} s^{-1} m^{-1} cm s^{-1}.

where H is the layer depth, shows that this is equivalent to a heat content change of some 97 W m^{-2} for the top 365 m. This is large compared to the average net annual surface flux of −4 W m^{-2} for the area [calculated using data from Josey et al. (1999)]. According to Jones and Leach (1999) the heat is probably supplied to the region by geostrophic transport in the NAC.

The depth-averaged eddy potential vorticity flux, $\overline{\mathbf{u}'q'}$, is shown in Fig. 9 superimposed on the mean potential vorticity and surface geostrophic velocity fields calculated relative to 1500 m (McCulloch and Leach 1997). In the north the flux is (6.4 ± 6.7, −3.7 ± 4.6) × 10^{-10} s^{-1} m^{-1} cm s^{-1} and in the south it is (4.9 ± 6.3, 6.2 ± 6.6) × 10^{-10} s^{-1} m^{-1} cm s^{-1}. The fluxes were calculated by combining the SeaSoar CTD and ADCP data. Because the sloping isopycnal surfaces pass through our relatively thin (365 m) layer within the area used for averaging (700 or 1000 km × 1500 km), it was not practical to average on these density surfaces, but instead depth levels were used. Potential vorticity is an inherently noisy parameter, and in Fig. 10 profiles of the zonal and meridional transports in the northern and southern halves of our area are shown. However, when depth-averaged, both zonal and meridional transports show values that are marginally significant. The fluxes show eastward zonal transport in both north and south areas but the meridional transports show southward values in the north and northward values in the south, implying a convergence toward the source

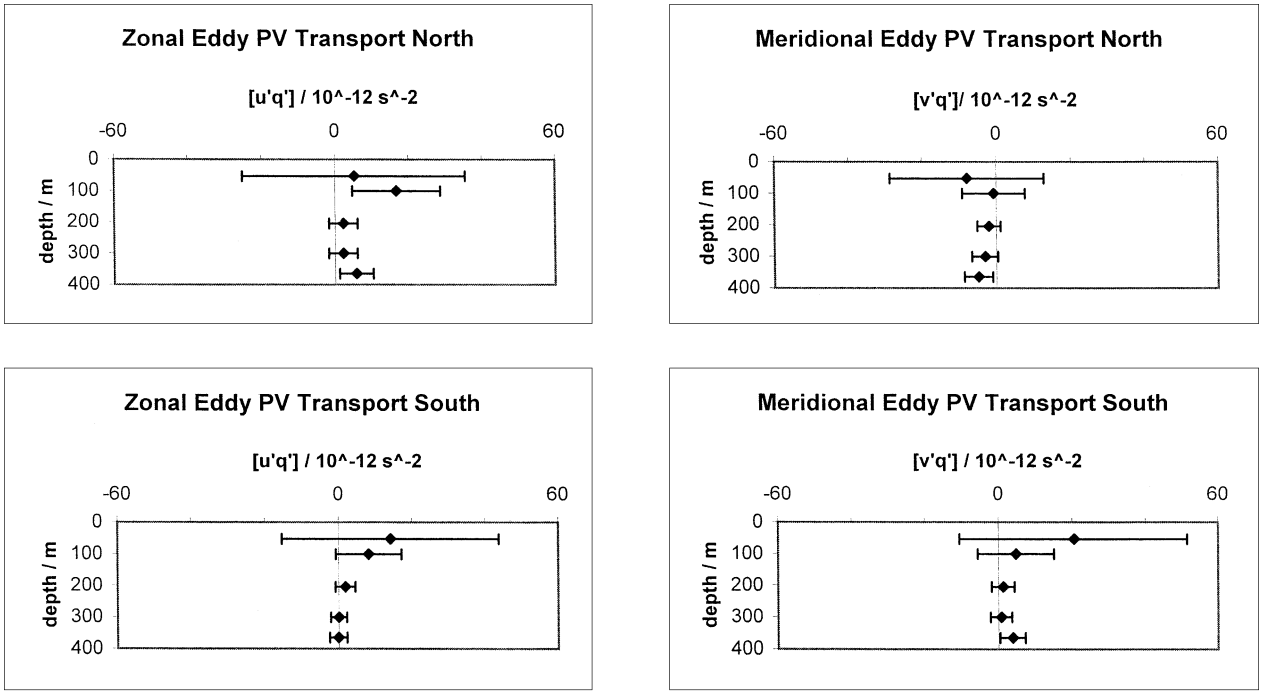

FIG. 10. Depth profiles of zonal and meridional eddy potential vorticity transport, $\overline{\mathbf{u}'q'}$, for the northern and southern halves of the area in units of 10^{-12} s^{-2} (or 10^{-10} m^{-1} s^{-1} cm s^{-1}). At any depth alone the transport is not significant; however, when depth averaged the situation improves marginally and the picture of eastward zonal transport in the north and south and southward meridional transport in the north and northward meridional transport in the south becomes more apparent.

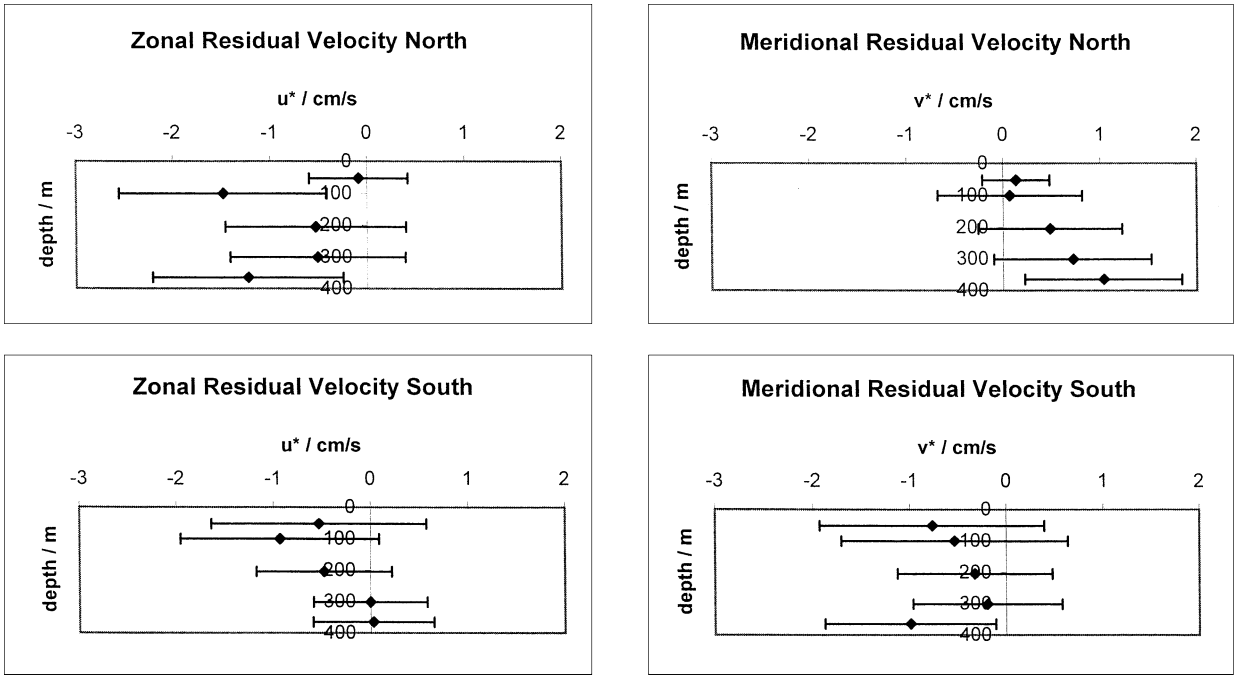

FIG. 11. Depth profiles of zonal and meridional residual or eddy transport velocity, $\mathbf{u}^* = -\overline{\mathbf{u}'q'}/\overline{q}$, for the northern and southern halves of the area in units of cm s^{-1}. While the individual values are not significant, taking all depths together shows westward zonal transport in both the north and south and northward transport in the north and southward transport in the north.

region of the eastern North Atlantic Central Water reported in Pollard et al. (1996). This should be expected—Pollard et al. (1996) describe how this region of deeper winter mixing is a source of mode water, which will have low potential vorticity, and how this water apparently spreads out toward the west. A westward spreading of low potential vorticity water will correspond to an eastward transport of (higher) potential vorticity.

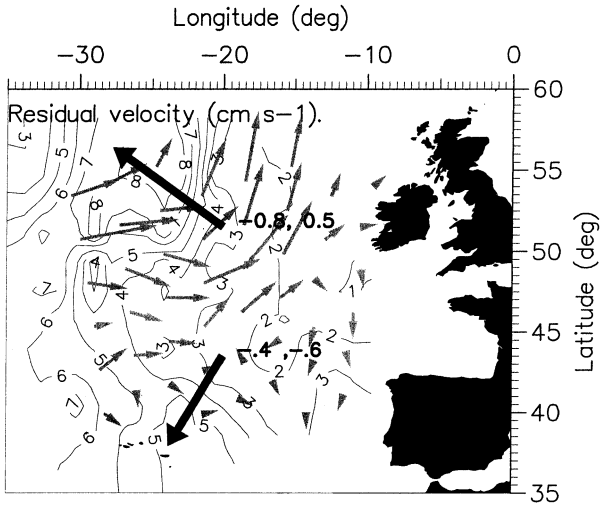

FIG. 12. The residual velocity or eddy transport velocity, $\mathbf{u}^* = -\overline{\mathbf{u}'q'}/\overline{q}$, (in cm s^{-1}) averaged over the top 365 m superimposed on the mean potential vorticity (in units of 10^{-10} m^{-1} s^{-1}) and surface geostrophic velocity fields relative to 1500 m. Note that the $\mathbf{u}^*$ vectors are drawn 10 times as large as the $\mathbf{u}_g$ vectors. In the south the residual velocity is toward the SW with a value of (-0.4 ± 0.4, -0.6 ± 0.4) cm s^{-1} or 0.7 cm s^{-1} to 214°. In the north it is toward the NW with a value of (-0.8 ± 0.4, 0.5 ± 0.3) cm s^{-1} or 0.9 cm s^{-1} to 302°.

To understand the magnitude of these potential vorticity transports it is easier to convert them to residual, eddy-induced velocities, given by

$$\mathbf{u}^* = -\overline{\mathbf{u}'q'}/\overline{q}.$$

(see, e.g., Edmon et al. 1980; Bowerman and Leach 1997; Treguier et al. 1997; Marshall et al. 1999). Profiles of $\mathbf{u}^*$ are shown in Fig. 11. As with the potential vorticity fluxes the values are rather noisy but when depth averaged become marginally significant. These depth-averaged values are shown in Fig. 12, superimposed on the mean potential vorticity field and surface geostrophic velocity fields. (It should be noted that in Fig. 12 the $\mathbf{u}^*$ vectors are drawn 10 times as large as the $\mathbf{u}_g$ vectors.) In the south this residual velocity is toward the SW with a value of (-0.4 ± 0.4, -0.6 ± 0.4) cm s^{-1} or 0.7 cm s^{-1} to 214°. In the north it is toward the NW with a value of (-0.8 ± 0.4, 0.5 ± 0.3) cm s^{-1} or 0.9 cm s^{-1} to 302°. The northern value shows the expected transport to the left of the jet in the Northern Hemisphere (Lee et al. 1997). This is a significant fraction of the mean speed of 6.5 cm s^{-1} and is perpendicular to the mean flow, which implies that the eddies are important for water mass transfer. The southern value shows the southwestward transport to be expected from the mode

TABLE 1. Summary of principal statistics for the northern and southern halves of the area and their ratios.

	$\lvert\bar{\mathbf{u}}\rvert$ (cm s^{-1})	EKE (cm^2 s^{-2})	$\lvert\overline{\mathbf{u}'T'}\rvert$ (K cm s^{-1})	$\lvert\overline{\mathbf{u}'q'}\rvert$ (10^{-10} s^{-1} m^{-1} cm s^{-1})	$\lvert\mathbf{u}^*\rvert$ (cm s^{-1})
North	6.5 ± 0.8	272 ± 11	5.5 ± 2.6	7.4 ± 5.7	0.9 ± 0.4
South	0.2 ± 0.8	205 ± 9	0.1 ± 1.5	7.9 ± 6.4	0.7 ± 0.4
South/north (%)	3	75	2	107	78

water spreading discussed by Pollard et al. (1996). Bowerman and Leach (1997) obtained a value of (−2.0, 2.9) cm s^{-1} for the region of the NAC, which is similar in magnitude and direction to the northern area values, bearing in mind their more restricted area and different averaging method.

4. Discussion

a. North–south contrasts

Comparison of the mean flow, EKE, and the eddy transports in the two halves of our region confirms the picture already reported by Bowerman and Leach (1997), whereby the EKE can be a significant fraction of its maximum value (see Fig. 4) well into regions where the mean flow (Fig. 9) or eddy heat transport (Fig. 7) become vanishingly small. Interestingly, the other parameters, which do not become small in these regions, are the eddy flux of potential vorticity (Fig. 9) and the closely related residual velocity (Fig. 12). These results are summarized in Table 1, which includes the ratio of values in the south expressed as a percentage of the values in the north; the mean flow and eddy heat transport in the south are only a few percent of their northern values, while the EKE in the south is only slightly reduced compared to the northern value and the eddy potential vorticity transport and residual velocity not significantly different from each other.

b. The size of the residual velocity

Simple consideration of the process of eddy production by baroclinic instability suggests that the residual or eddy transport velocity should have the speed of one eddy scale per baroclinic life cycle. James (1994) gives the growth rate of the baroclinic disturbance, ω_i, as

$$\omega_i = 0.31\frac{\Delta U}{L_R},$$

where L_R is the Rossby radius. If it is then assumed that the residual or eddy-induced transport speed, V^*, is L_R/τ, where $\tau = 1/\omega_i$, then

$$V^* = \frac{L_R}{\tau} = L_R\omega_i = 0.31\Delta U.$$

This implies that the eddy-induced speed should be about 31% of the top-to-bottom velocity difference of the mean flow or, roughly speaking, 31% of the flow at the surface under typical oceanic conditions, assuming the flow at depth is relatively small. The results presented in this paper show the residual speed to be perhaps less than this in the northern half of the area (0.9 cm s^{-1}/6.5 cm s^{-1} ∼ 14 ± 8%), though the errors are not small and it should be remembered that here we have averaged over a relatively large area that includes some areas away from the jet. Bowerman and Leach (1997) calculated that the residual speed in the NAC was about 3 cm s^{-1} with a mean flow of some 10 cm s^{-1}, which comes nearer to the simple theoretical consideration of 31%.

In the southern half of the area we have the different situation that the residual speed may even be larger than the mean speed (0.7 ± 0.4 cm s^{-1} compared to 0.2 ± 0.8 cm s^{-1}). This implies that either the simple-minded relationship between V^* and ΔU is flawed or that physical processes other than baroclinic instability of a jet are responsible for the eddies. Some authors, such as Müller and Frankignoul (1981) and White and Heywood (1995), have hypothesized that away from strong currents winds may be important, though without specifying the details of a mechanism for the transfer of energy. The residual velocity is merely a correlation between the velocity and potential vorticity fluctuations, and its existence does not necessarily imply the existence of baroclinic instability. Any other phenomenon, such as internal waves or baroclinic Rossby waves, might, under the right conditions, lead to a rectified volume transport analogous to the Stokes drift for surface waves. In numerical calculations of mesoscale eddies with localized forcing regions and no bottom topography (e.g., Lee and Leach 1996) the rest of the channel, or basin, fills with EKE spreading from the source region in the jet, but it is not clear whether this is also the cause of EKE in oceanic regions with weak gradients where there are other competing mechanisms, such as wind forcing, as discussed above.

c. Balancing the volume fluxes

It is not initially obvious how the volume flux implied by the residual velocity is supplied. There seem to be three options, which are indicated schematically in Fig. 13.

1) *Option A*: The upwelling, W^*, that would be implied by the divergence of the eddy-induced velocity, $W^* = H\lvert\partial v^*/\partial y\rvert$, corresponds to 40 m yr^{-1} for an arbitrary depth scale, H, of 100 m (arrow A in the schematic Fig. 13). This is of the same order as

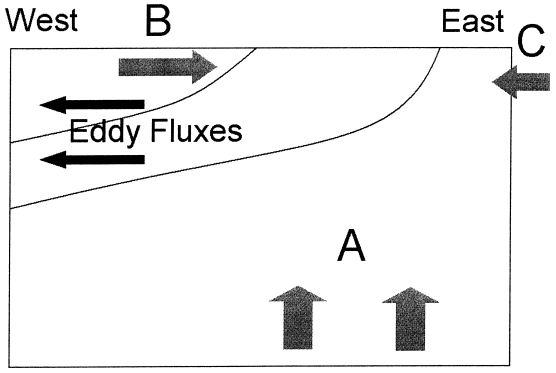

FIG. 13. Schematic zonal section through the area with isopycnal spacing thinning toward the west. Possible sources of water required to balance the divergence from the source region of the eastern North Atlantic Central Water are shown: (a) eddy-induced upwelling, (b) influx at the surface as required by Marshall (1997) but for which there is no observational evidence, (c) inflow from the eastern boundary.

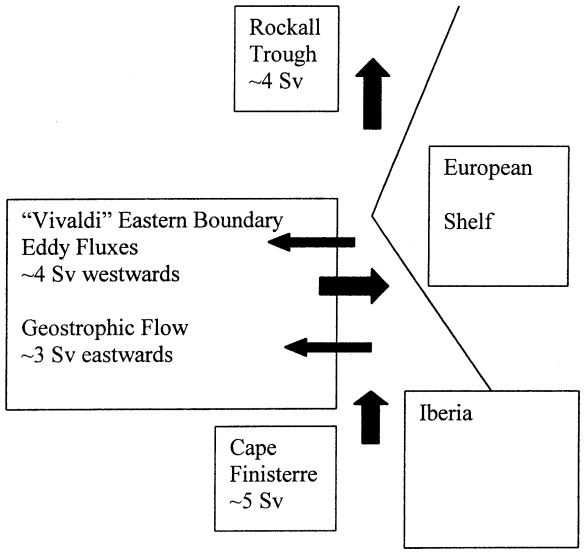

FIG. 14. Schematic summarizing possible flows and fluxes along, into, and out of the eastern boundary required to balance the westward eddy volume flux in the eastern midlatitude North Atlantic. Thin arrows represent eddy fluxes and fat arrows geostrophic flows; about 5 Sv flow northward at Cape Finisterre losing about 4 Sv westward by eddy fluxes but gaining about 3 Sv from geostrophic flows leaving about 4 Sv flow northward into the Rockall Trough.

Ekman pumping (Isemer and Hasse 1987), though Ekman pumping and suction are likely to be a maximum in the centers of the subtropical and subpolar gyres and not here in our survey area on the boundary between the gyres. This means that an eddy-induced upwelling could potentially be as important as Ekman pumping for the vertical transport of water properties and dissolved substances of biogeochemical significance. However, it is not clear that this is the right model for our region; Marshall (1997) predicts convergence not divergence.

2) *Option B*: Marshall (1997) has considered eddy fluxes driven by isolated regions of cooling. He shows that there should be an influx of warm water near the surface and an efflux of cold water at depth, which makes sense seen thermodynamically. In our case there is an outflow of about 1 cm s^{-1} over the top 400 m. To balance this in the way described by Marshall (1997) there would need to be an even shallower inflow of, say, 10 cm s^{-1} over 40 m (arrow B in Fig. 13). No such flow is apparent in our ADCP data (section 3a above) nor is there in the depth profiles of **u*** (Fig. 11). Neither is there evidence of strong climatological Ekman convergence in this region (Isemer and Hasse 1987; Josey et al. 1999), though curiously there seems to have been a synoptic convergence in May 1991 (McCulloch and Leach 1997). However, it is not clear that this is the right model for our region either as the region of cooling is not necessarily closed to the east.
3) *Option C*: The only other source of water that could diverge from this region, if it cannot come from above or below, is the eastern boundary (arrow C in Fig. 13). This is a complex issue; the southward-sloping isopycnals in this dataset (Pollard et al. 1996) imply an *eastward* geostrophic transport. For our range of latitudes this can be estimated from Bord Est data (Arhan et al. 1994). We obtain about +3 Sv for their layer 1 shallower than $\sigma_\theta = 27.25$ kg m^{-3}, or roughly 500 m. Cunningham (2000), in a Bernoulli inverse of the deep CTDs associated with this dataset, estimates +6 (±5) Sv moving eastward between 42° and 56°N across the eastern boundary of his inversion box in a layer shallower than $\sigma_2 = 36.873$ kg m^{-3}, which includes the Mediterranean Water. Our *westward* eddy fluxes imply a transport of about -0.6 cm $s^{-1} \times 15°$ lat $\times$ 365 m $= -3.7$ Sv. Estimates of the northward eastern boundary current transport near Cape Finisterre are about 4.9 Sv (Mazé et al. 1997). Farther north, in the Rockall Trough, Holliday et al. (2000) have calculated a mean net northward transport of about 3.7 (±2.4) Sv, which, though strictly for the whole water column, must in practice be for the upper layers as the trough is closed to the north at depth about 500 m by the Wyville–Thompson Ridge. Could it then be that, if there is little significant change in the eastern boundary transport between Cape Finisterre and the Rockall Trough, the eastward geostrophic transport into the boundary between these latitudes is largely balanced by a westward mass flux by the eddy field? See Fig. 14 for a summary of these possible fluxes.

5. Conclusions

The transports by mesoscale eddies in the eastern North Atlantic show a significant poleward transport of heat in the region of the NAC. They also show a convergent eddy flux of potential vorticity toward the

source region of the eastern North Atlantic Central Water. The implied residual velocity or eddy-induced mass transport is northwestward across the North Atlantic Current. In the region of weak mean currents between the North Atlantic Current and the Azores Current the eddy-induced mass transport is southwestward away from the source region of the eastern North Atlantic Central Water. While in the north of our region the mean flow and eddy heat transport are significant, they are both small in the south. In contrast the EKE is only slightly diminished in the south, being 75% of the northern values, and eddy potential vorticity flux or residual flow are of equal magnitude. Balancing the mass flux implied by the eddy-induced residual velocities is more difficult. A variety of options have been considered, perhaps the most promising of which suggests the westward eddy volume flux is balanced partly by an eastward geostrophic flow and partly by flow leaving the northward flowing eastern boundary current.

Acknowledgments. The data for this paper were collected during Cruises 58 and 59 of RRS *Charles Darwin*, and we should like to thank the captain and crew for their support. We should also like to thank colleagues at the former James Rennell Centre for Ocean Circulation, now at the Southampton Oceanography Centre, for their support with the data collection and processing both during and after the cruise. SJB and MEM were supported by grants from the Natural Environment Research Council. We also thank Ric Williams, David Marshall, and Martin Visbeck for useful discussions.

REFERENCES

Arhan, M., A. Colin de Verdiére, and L. Mémery, 1994: The eastern boundary of the subtropical North Atlantic. *J. Phys. Oceanogr.,* **24,** 1295–1316.

Bowerman, S. J., and H. Leach, 1997: Eddies in the north east Atlantic: Statistics from observations from a moving ship. *J. Geophys. Res.*, **102,** 23 041–23 062.

Brügge, B., 1995: Near-surface mean circulation and kinetic energy in the central North Atlantic from drifter data. *J. Geophys. Res.,* **100,** 20 543–20 554.

Cromwell, D., P. G. Challenor, and A. L. New, 1996: Persistent westward flow in the Azores Current as seen from altimetry and hydrography. *J. Geophys. Res.,* **101** (C5), 11 923–11 933.

Cunningham, S. A., 2000: Circulation and volume flux of the North Atlantic using synoptic hydrographic data in a Bernoulli inverse. *J. Mar. Res.,* **58,** 1–35.

——, and Coauthors, 1992: SeaSoar CTD, fluorescence and scalar irradiance data from RRS *Charles Darwin* Cruises 58/59, NE Atlantic (Vivaldi 91). Institute of Oceanographic Sciences Deacon Laboratory Rep. No. 299, 48 pp.

Dietrich, G., K. Kalle, W. Krauss, and G. Siedler, 1975: *Allgemeine Meereskunde.* Gebr. Borntraeger, xii + 593 pp.

Edmon, H. J., B. J. Hoskins, and M. E. McIntyre, 1980: Eliassen–Palm cross sections for the troposphere. *J. Atmos. Sci.,* **37,** 2600–2616; Corrigendum, *J. Atmos. Sci.,* **38,** 1115.

Ellett, D. J., 1993: The north-east Atlantic: A fan-assisted storage heater? *Weather,* **48,** 118–126.

Fischer, J., H. Leach, and J. D. Woods, 1989: A synoptic map of isopycnic potential vorticity in the seasonal thermocline. *J. Phys. Oceanogr.,* **19,** 519–531.

Gent, P. R., and J. C. McWilliams, 1990: Isopycnal mixing in ocean circulation models. *J. Phys. Oceanogr.,* **20,** 150–155.

Griffiths, G., and Coauthors, 1992: CTD oxygen, tracer and nutrient data from RRS *''Charles Darwin''* Cruises 58/59 in the NE Atlantic as part of Vivaldi'91. Institute of Oceanographic Sciences Deacon Laboratory Rep. 296, 51 pp.

Helland-Hansen, B., and F. Nansen, 1926: The eastern North Atlantic. *Geofys. Publ.,* **4** (2), 76 pp.

Heywood, K. J., E. L. McDonagh, and M. A. White, 1994: Eddy kinetic energy of the North Atlantic subpolar gyre from satellite altimetry. *J. Geophys. Res.,* **99,** 22 525–22 539.

Holliday, N. P., R. T. Pollard, J. F. Read, and H. Leach, 2000: Water mass properties and fluxes in the Rockall Trough; 1975 to 1998. *Deep-Sea Res.,* **47A,** 1303–1332.

Hoskins, B. J., I. N. James, and G. H. White, 1983: The shape, propagation and mean-flow interaction of large-scale weather systems. *J. Atmos. Sci.,* **40,** 1595–1612.

Isemer, H.-J., and L. Hasse, 1987: *The Bunker Climate Atlas of the North Atlantic Ocean.* Vol. 2, *Air–Sea Interactions,* Springer Verlag, vii + 252 pp.

——, J. Willebrand, and L. Hasse, 1989: Fine adjustment of large scale air–sea energy flux parameterizations by direct estimates of ocean heat transport. *J. Climate,* **2,** 1173–1184.

James, I. N., 1994: *Introduction to Circulating Atmospheres.* Cambridge University Press, xxii + 422 pp.

Jones, I. D., and H. Leach, 1999: Isopycnic modelling of the North Atlantic heat budget. *J. Geophys. Res.,* **104,** 1377–1392.

Josey, S. A., E. C. Kent, and P. K. Taylor, 1999: New insights into the ocean heat budget closure problem from analysis of the SOC air–sea flux climatology. *J. Climate,* **12,** 2856–2880.

Krauss, W., 1986: The North Atlantic Current. *J. Geophys. Res.,* **91** (C4), 5061–5074.

——, and R. H. Käse, 1984: Mean circulation and eddy kinetic energy in the eastern North Atlantic. *J. Geophys. Res.,* **89,** 3407–3415.

Leach, A., 1984: Some correlations between the large-scale meridional momentum transport and zonal mean quantities. *J. Atmos. Sci.,* **41,** 236–245.

Lee, M.-M., and H. Leach, 1996: Eliassen–Palm flux and eddy potential vorticity flux for a nonquasigeostrophic time-mean flow. *J. Phys. Oceanogr.,* **26,** 1304–1319.

——, D. P. Marshall, and R. G. Williams, 1997: On the eddy transfer of tracers: Advective or diffusive? *J. Mar. Res.,* **55,** 483–505.

Le Groupe Tourbillon, 1983: The Tourbillon Experiment: A study of a mesoscale eddy in the eastern North Atlantic. *Deep-Sea Res.,* **30A,** 475–511.

Marshall, D., 1997: Subduction of water masses in an eddying ocean. *J. Mar. Res.,* **55,** 201–222.

——, R. G. Williams, and M.-M. Lee, 1999: The relation between eddy-induced transport and isopycnic gradients of potential vorticity. *J. Phys. Oceanogr.,* **29,** 1571–1578.

Mazé, J. P., M. Arhan, and H. Mercier, 1997: Volume budget of the eastern boundary layer off the Iberian Peninsula. *Deep-Sea Res.,* **44A,** 1543–1574.

McCulloch, M. E., and H. Leach, 1997: Seasonal heat and fresh water budgets of the upper ocean in the north-east Atlantic. *Quart. J. Roy. Meteor. Soc.,* **123,** 767–784.

Müller, P., and C. Frankignoul, 1981: Direct atmospheric forcing of geostrophic eddies. *J. Phys. Oceanogr.,* **11,** 287–308.

Onken, R., 1993: The Azores Countercurrent. *J. Phys. Oceanogr.,* **23,** 1638–1646.

Paillet, J., and H. Mercier, 1997: An inverse model of the eastern North Atlantic general circulation and thermocline ventilation. *Deep-Sea Res.,* **44A,** 1293–1328.

Pollard, R. T., H. Leach, and G. Griffiths, 1991: RRS *Charles Darwin* Cruises 58 and 59. Institute of Oceanographic Sciences Deacon Laboratory Cruise Rep. 228, 49 pp.

——, M. J. Griffiths, S. A. Cunningham, J. F. Read, F. F. Pérez, and

A. F. Ríos, 1996: Vivaldi 1991—A study of the formation, circulation and ventilation of eastern North Atlantic Central Water. *Progress in Oceanography,* Vol. 37, Pergamon, 167–192.

Richardson, P. L., 1983: Eddy kinetic energy in the North Atlantic from surface drifters. *J. Geophys. Res.,* **88,** 4355–4367.

Stammer, D., and C. Wunsch, 1999: Temporal changes in eddy energy of the oceans. *Deep-Sea Res.,* **46B,** 77–108.

Tai, C.-K., and W. B. White, 1990: Eddy variability in the Kuroshio Extension as revealed by *Geosat* altimetry: Energy propagation away from the jet, Reynolds' stress and seasonal cycle. *J. Phys. Oceanogr.,* **20,** 1761–1777.

Treguier, A. M., I. M. Held, and V. D. Larichev, 1997: Parameterization of quasigeostrophic eddies in primitive equation ocean models. *J. Phys. Oceanogr.,* **27,** 567–580.

White, M. A., and K. J. Heywood, 1995: Seasonal and interannual changes in the North Atlantic subpolar gyre from *Geosat* and TOPEX/POSEIDON altimetry. *J. Geophys. Res.,* **100,** 24 931–24 941.